Polymer 50 (2009) 6111–6120

Contents lists available at ScienceDirect

Polymer

journal homepage: www.elsevier.com/locate/polymer

A delicate ionizable-group effect on self-assembly and thermogelling of amphiphilic block copolymers in water

Guangtao Chang, Lin Yu, Zigang Yang, Jiandong Ding*

Key Laboratory of Molecular Engineering of Polymers of Ministry of Education, Department of Macromolecular Science, Laboratory of Advanced Materials, Fudan University, Shanghai 200433, China

ARTICLE INFO

Article history:
Received 24 July 2009
Received in revised form
12 October 2009
Accepted 15 October 2009
Available online 21 October 2009

Keywords:
Hydrogel
Self-assembly
Block copolymer

ABSTRACT

A carboxyl-capped PLGA–PEG–PLGA block copolymer (PLGA: poly(D,L-lactic acid-*co*-glycolic acid), PEG: poly(ethylene glycol)) was synthesized, and its self-assembly and thermogelling behaviors in water were studied at different pH values. While the aqueous solution of the virgin PLGA–PEG–PLGA block copolymer with the composition in this paper did not undergo sol–gel transition, that of the end-capped derivative exhibited four macroscopic states, sol, turbid sol, physical gel, and precipitate, dependent upon temperature and pH. Especially between pH 4.5 and 5.0, a concentrated aqueous system underwent sol–gel-(turbid sol)-precipitate transitions upon increase of temperature. Complex of dissociation constant pK_a of weak-acid groups on the micelle surfaces was illustrated. Dynamic light scattering, hydrophobic dye solubilization, transmission electron microscopy, NMR, and potentiometric titration were used to examine the relationship between ionization of the end groups of the polymer chains on the molecular level, micellization of the amphiphilic block copolymers on the supermolecular level, and physical gelation on the macroscopic level. The present research reveals the complex of the multi-scale self-assembly of amphiphilic polymer ionomers in a selective solvent.

1. Introduction

Over the past few decades, much interest has been devoted to the self-assembly behaviors of amphiphilic polymers [1–6]. While in many cases amphiphilic copolymers are aggregated into micelles due to the hydrophobic association in water, a part of copolymers containing blocks of poly(ethylene glycol) (PEG) etc. even further self-assemble into physical hydrogels upon a concentration above critical gelation concentration (CGC) and a temperature above critical gelation temperature (CGT) [7–23]. Those physical gels are very promising in biomedical applications such as sustained drug release and tissue engineering [8,18,24–28]. Recently, attention has been paid upon a kind of biodegradable and biocompatible copolymers composed of PEG and polyesters, especially triblock copolymers of PEG and poly(D,L-lactic acid-*co*-glycolic acid) (PLGA), PLGA–PEG–PLGA [8,11,17,29–31]. Under an appropriate composition, the copolymers of polyether and polyester could exhibit three states, sol, gel and precipitate, depending upon concentration and temperature.

This paper will examine both pH- and temperature-dependence of self-assembly of a PLGA–PEG–PLGA derivative. Carboxy groups are introduced to the ends of PLGA–PEG–PLGA chains with the synthesis route presented in Fig. 1. While the carboxyl effects on micellization in the case of "ionomers" of other polymers have been investigated [32–34], its effect on a potential thermogelling system remains as an interesting fundamental issue. It seems that the self-assembly behaviors of carboxyl-capped PLGA–PEG–PLGA may be influenced by the ionization/deionization balance as well as hydrophilicity/hydrophobicity balance. We surprisingly found that introduction of one or two charges into a small fraction of polymers led to a significant change of the self-assembled macroscopic states. The rich physics constitutes the theme of the present paper.

2. Experimental section

2.1. Materials

PEG were purchased from Fluka, and stannous 2-ethylhexanoate (stannous octoate), from Sigma. D,L-lactide (LA) and glycolide (GA) were obtained from Purac and used without further treatment. All other chemicals were of reagent grade and used as purchased without further purification.

* Corresponding author. Tel.: +86 21 65643506; fax: +86 21 656402931.
E-mail address: jdding1@fudan.edu.cn (J. Ding).

0032-3861/$ – see front matter © 2009 Elsevier Ltd. All rights reserved.
doi:10.1016/j.polymer.2009.10.036

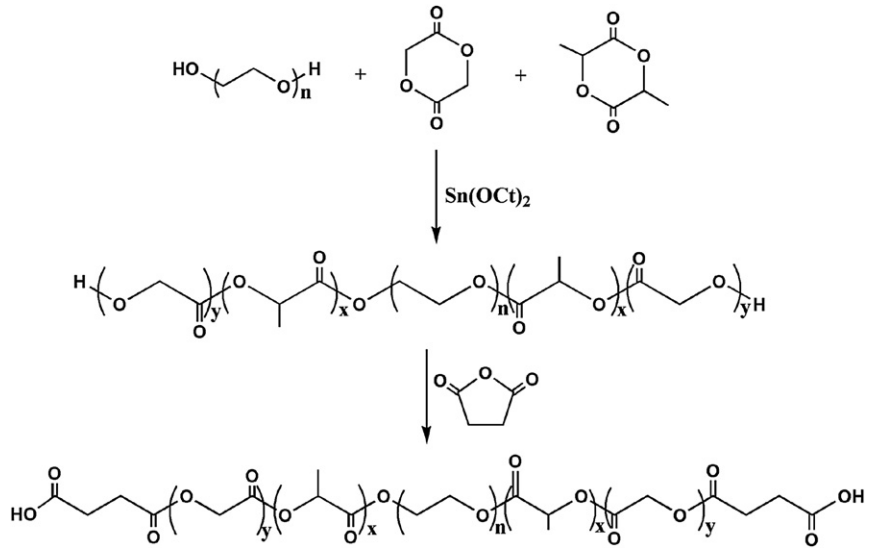

Fig. 1. Synthesis route of PLGA–PEG–PLGA and its carboxyl-capped derivative denoted as HOOC–PLGA–PEG–PLGA–COOH.

2.2. Synthesis of carboxyl-capped PLGA–PEG–PLGA

PLGA–PEG–PLGA triblock copolymers were synthesized following the method described previously [8,29,30,35]. Briefly, the ring-opening polymerization of LA and GA was performed in the presence of PEG, and stannous octoate was used as catalyst. The copolymer was collected after precipitated in water at 80 °C. Then, the virgin copolymer was end-capped with the route shown in Fig. 1. PLGA–PEG–PLGA (15 g), succinic anhydride (3.3 g), pyridine (2 mL), and dichloromethane (120 mL) were added to a dry three-neck round-bottom flask equipped with a condenser, and refluxed for 48 h. The reaction solution was stored in a refrigerator at −20 °C for several hours. The filtered solution was precipitated in diethyl ether, further purified through dissolving in diluted hydrochloric acid, and re-precipitated at 80 °C in water to wipe off the remaining succinic anhydride and pyridine residues. The precipitate was freeze-dried for 48 h.

2.3. Gel permeation chromatography (GPC)

GPC in an Agilent 1100 apparatus with a differential refractometer as a detector was used to measure the molecular weights (MWs) of polymers and MW distribution. Tetrahydrofuran was used as an eluting solvent at a flow rate of 1.0 mL/min at 35 °C. Polystyrene (PS) was used as MW standard.

2.4. NMR spectrometry

^{1}H NMR and ^{13}C NMR measurements were performed in a Bruker DMX500 spectrometer at resonance frequency of 500 MHz. The pH in the NMR experiments (pD) was adjusted by NaOD or DCl solution in D_2O. The relation between pD and pH is pD = pH + 0.4 [36,37].

2.5. Poentiometric titration

After 10 mL of 2 wt% carboxyl-capped copolymer solution was prepared, the solution was titrated with 0.1 M NaOH at 20.5 °C under argon atmosphere. The physiological saline solution with 0.9 wt% NaCl was used as well as pure water. The pH and the volume of added NaOH solution were recorded to obtain the titration profile. 0.2 wt% acrylic acid was also prepared and titrated with 0.4 M NaOH. The corrected curve was fitted with Henderson–Hasselbalch (HH) equation to obtain the apparent pK_a and the beginning point and end point of the titration curve.

2.6. Cloud point

Cloud point was judged by absorption at 650 nm versus temperature. Each sample was dissolved in phosphate buffered saline (PBS) solution (1 L PBS containing 8.0 g NaCl, 0.2 g KH_2PO_4, 0.2 g KCl, 2.9 g $Na_2HPO_4{\cdot}12H_2O$) and adjusted by 4 M HCl or 4 M NaOH to obtain given pH values. Samples were immerged in a water bath at a fixed temperature for 15 min, and then its absorbency at 650 nm was measured quickly. The temperature corresponding to a drastic increase of absorbance was determined as the cloud point.

2.7. Test tube inverting examination

Sol-to-gel transition temperatures were recorded by the test tube inverting method with a temperature increment of 1 °C per step. A PBS solution was adjusted by 4 M HCl or 4 M NaOH to obtain different pH values. After equilibration at 4 °C for 48 h, the vials containing samples were immersed in a water bath equilibrated at each given temperature for 15 min. The sol–gel transition was examined by inverting the vial, and the sample was regarded as a gel in the case of no flow within 30 s.

2.8. Dynamic rheological analysis

The sol–gel transition of the copolymer aqueous solution was also detected in a dynamic strain-controlled rheometer (ARES Rheometer Scientific) with a Couette cell (Couette diameter, 34 mm; bob diameter, 32 mm; bob height, 33.3 mm; bob gap, 2 mm). The temperature was adjusted with accuracy of ±0.05 °C by an environmental controller (Neslab). Cold polymer solutions were carefully transferred into the Couette cell and overlaid with a thin layer of low-viscosity silicone oil (100 cp at room temperature) to minimize solvent evaporation. During temperature sweeping, strain amplitude was set at an appropriate value determined from pre-tests to achieve both the linearity of viscoelasticity and

a sufficient torque for suitable data collection. The heating rate was set as 0.5 °C/min, whereas the angular frequency was 10 rad/s. The viscosity was calculated by $\eta = (G'^2 + G''^2)^{1/2}/\omega$. Here, ω, G' and G'' denote frequency, storage modulus and dissipative modulus, respectively.

2.9. Critical micelle concentration (CMC)

The CMC values were determined by the hydrophobic dye solubilization method [7,21]. 150 μL of 0.4 mM 1,6-diphenyl-1,3,5-hexatriene (DPH) methanol solution was injected into PBS solution, and then stirred at room temperature for 4 h to evaporate the methanol. The PBS solution containing dye was divided into two parts with pH adjusted to 3.0 and 9.0. A 1.0 wt% polymer solution was also adjusted to pH 3.0 and 9.0, and then diluted into two series of concentrations with the corresponding PBS. The absorption spectra of these samples were recorded from 250 to 450 nm at 25 °C. Partitioning of DPH into a hydrophobic domain such as the core of a micelle results in stronger absorbance at 337, 356, and 376 nm. The CMC was estimated as the crossing point when the extrapolation of the absorbance at 376 nm with respect to that at 400 nm was plotted against the logarithmic polymer concentration. The absorption difference was used to compensate the scattering effect.

2.10. Dynamic light scattering (DLS)

DLS measurements were performed in a light scattering spectrophotometer (Autosizer 4700, Malvern) with a vertically polarized incident beam at 532 nm supplied by an argon-ion laser. A scattering angle of 90° was detected in this study. Before measurements, all samples were treated with a 0.45-μm filter (Millipore). The Stocks-Einstein equation was employed to calculate the hydrodynamic radius of the micelles. Polymers were resolved in PBS, and medium pH was adjusted by addition of 4 M NaOH or 4 M HCl. Each sample was equilibrated for 10 min at every set temperature.

2.11. Transmission electron microscopy (TEM)

TEM was performed in a JEM-2011 electronic microscope. The sample was prepared by placing 5 μL of 1 wt% carboxyl-capped PLGA–PEG–PLGA solution at a certain pH solution on copper grids coated with a thin carbon film and drying the solution at the room temperature. No staining was performed. The sample was observed on an electronic microscope at an accelerating voltage of 200 kV.

3. Results

3.1. Synthesis of the polymer and characterization of the chemical structure

PLGA–PEG–PLGA triblock copolymers were synthesized via ring-opening copolymerization of LA and GA using PEG (1500 Da) as a macroinitiator. Carboxyl-capped triblock copolymers were obtained by further ring-opening of succinic anhydride in the presence of PLGA–PEG–PLGA with the synthesis route shown in Fig. 1. The resulting ^{1}H NMR spectra of the triblock copolymers and the carboxyl-capped copolymers are presented in Fig. 2. The new proton signal shown at 2.73 ppm in the upper spectrum was assigned to the methylene protons (–CH_2CH_2–) of the succinyl unit. The MW and composition were confirmed from ^{1}H NMR using PEG (1500 Da) as standard, the MW distribution was obtained from GPC relative to the PS standard. The carboxyl substitution was about 100%. The data were summarized in Table 1.

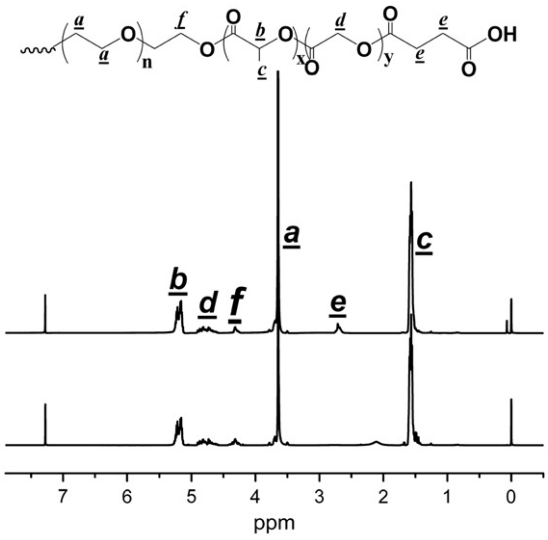

Fig. 2. ^{1}H NMR spectra of PLGA–PEG–PLGA (lower) and HOOC–PLGA–PEG–PLGA–COOH (upper).

3.2. The pK_a titration

The degree of ionization α is defined as

$$\alpha(\mathrm{pH}) \equiv \frac{\left[\mathrm{COO}^-\right]}{[\mathrm{COOH}] + \left[\mathrm{COO}^-\right]}, \tag{1}$$

where [COOH] and [COO^-] are concentrations of deionized and ionized carboxyls, respectively. The pK_a of the weak acid, the carboxyl-capped PLGA–PEG–PLGA is defined as

$$\mathrm{p}K_\mathrm{a} \equiv -\lg K_\mathrm{a},\ K_\mathrm{a} \equiv \frac{\left(\mathrm{COO}^-\right)\left(\mathrm{H}^+\right)}{(\mathrm{COOH})}, \tag{2}$$

where K_a is the equilibrium dissociation constant, (H^+), (COOH) and (COO^-) are activities of medium proton, deionized and ionized carboxyls, respectively. Neglecting the difference between activity and concentration under assumption of the so-called ideal solution, α is theoretically related to pK_a and pH via the following equation

$$\alpha = \frac{1}{1 + 10^{\mathrm{p}K_\mathrm{a} - \mathrm{pH}}}. \tag{3}$$

The potentiometric titration experiment was performed to determine α of the carboxyl-capped PLGA–PEG–PLGA under a given pH, following Winnik et al. in their studies of dissociation properties of poly(*n*-butyl methacrylate) in water [38]. Both water and the aqueous solution of carboxylated polymers were slowly titrated at argon atmosphere. The subtraction of data between the

Table 1
Basic characterization of the synthesized PLGA–PEG–PLGA and its carboxyl-capped derivative.

Copolymer M_n[a]	LA/GA (mol/mol)[a]	Carboxyl substitution percent[a]	M_w/M_n[b]
PLGA–PEG–PLGA 1330-1500-1330	5.47/1	\	1.19
HOOC–PLGA–PEG–PLGA–COOH 102-1330-1500-1330-102	5.47/1	102%	1.20

[a] The number-average MW M_n and LA/GA ratio were obtained from ^{1}H NMR.
[b] The MW distribution denoted by weight-average MW over M_n, M_w/M_n was obtained from GPC.

experimental group and the blank group was used to determine the net consumption by the sample including the start and end points in titration, denoted as V_0 and V_{end}. Then α is simply obtained by

$$\alpha(\mathrm{pH}) = \frac{V(\mathrm{pH}) - V_0}{V_{end} - V_0}. \quad (4)$$

The pK_a could be further determined as the pH at $\alpha = 0.5$, denoted as pK_a(0.5) by us in this paper.

The titration results are shown in Fig. 3. We also introduced two points a bit different from Winnik et al. [38]. First, since it is not very precise to determine V_0 and V_{end} simply from the subtraction

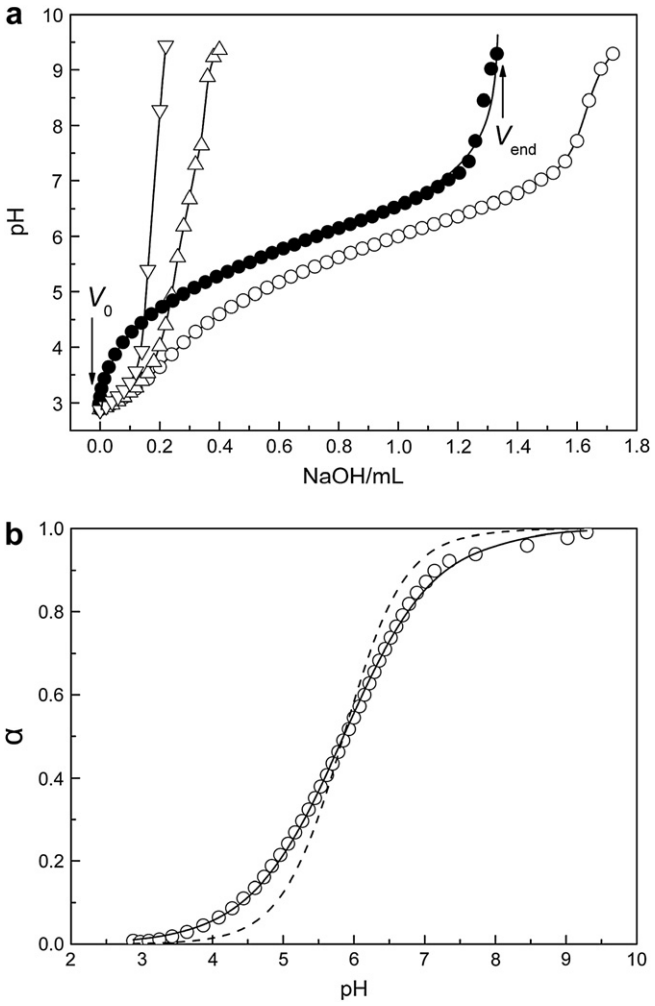

Fig. 3. (a) Suspension pH versus V, volume of 0.1 M NaOH solution presenting the titration curve of 10 mL of water or polymer aqueous solutions at 20.5 °C. The hollow circles (○) represent data of the 2 wt% carboxyl-capped PLGA–PEG–PLGA in 0.9 wt% NaCl solution; the hollow upper triangles (△) represent data of the 2 wt% PLGA–PEG–PLGA in 0.9 wt% NaCl solution; the hollow inverted triangles (▽) represent data of the 0.9 wt% NaCl solution. The filled circles (●) show the titration curve of the aqueous solution of HOOC–PLGA–PEG–PLGA–COOH after correction using 2 wt% PLGA–PEG–PLGA as a blank. The number of filled circles is the same as that of hollow circles. The datum of each filled circle under a given pH was obtained by the addition volume in the experimental group minus the calculated value of the control group under the same pH, and the calculation was done by a linear insertion between the two neighbor data points of the control group. The line corresponding to the filled circles is a fit by HH equation, resulting in pK_a(0.5) = 5.85 ± 0.01, n = 0.66 ± 0.01, V_0 = −0.011 ± 0.006 mL, V_{end} = 1.342 ± 0.008 mL; the lines in other three cases are just for guidance of eyes. (b) Degree of ionization (α) of 2 wt% carboxyl-capped PLGA–PEG–PLGA in 0.9 wt% NaCl solution as a function of pH. The hollow circles (○) represent the experimental data obtained by equation (4); the solid line is a fit with HH equation (similar to equation (5)) resulting in pK_a(0.5) = 5.85 ± 0.01. The dashed line represents the theoretical curve under the ideal condition (equation (3)) when pK_a(0.5) = 5.85.

data as shown in Fig. 3a, we employed the HH equation [39]. The equation in this case could be written as

$$V = V_0 + \frac{V_{end} - V_0}{1 + 10^{n[\mathrm{p}K_a(0.5) - \mathrm{pH}]}}, \quad (5)$$

where n is an adjustable constant and related to the sharpness of the transition. This equation fitted our titration data very well. Secondly, we took the corresponding aqueous solution of the virgin polymer without carboxyl capping as control instead of just water. The resultant pK_a(0.5) after correcting with the virgin triblock copolymer in the physiological saline solution was 5.85 ± 0.01 (n = 0.66 ± 0.01), and the pK_a(0.5) after correcting with water (actually 0.9 wt% NaCl solution) was 5.85 ± 0.01 (n = 0.67 ± 0.01). So, taking water as blank control as done by Winnik et al. is satisfactory at least for our sample under such a measurement condition. We also confirmed that no correction might lead to deviation because pK_a(0.5) = 5.76 ± 0.03 (n = 0.52 ± 0.02) by fitting just the initiate titration curve of HOOC–PLGA–PEG–PLGA–COOH in the physiological saline solution. Comparison between the experimental titration data and the theoretical curve expressed by equation (3) (Fig. 3b) illustrates that our sample is not ideal and thus those ionizable groups must interact with each other.

3.3. Physical gelling of the carboxyl-capped PLGA–PEG–PLGA in water

The initial PLGA–PEG–PLGA triblock copolymers of the composition shown in Table 1 were well soluble in PBS up to concentration of 20 wt%. The sol–gel transition of the aqueous solution of the virgin copolymer of the composition in this study was observed at none of pH values and temperatures examined by us, because the PLGA block is not sufficiently long. The state of the virgin block copolymer as functions of pH and temperature is shown in Fig. 4a. The concentrated carboxyl-capped PLGA–PEG–PLGA block copolymer aqueous solutions exhibited, however, thermogelling at a low pH. This is not unreasonable, because the end-capping enhances hydrophobicity of the copolymer and this kind of block copolymer has a very subtle end-group effect on macroscopic physical gelation as reported previously by our group [30,35], but just non-ionizable alkyl groups were introduced into the end groups. Recently, Kim et al. reported that alkyl end groups might also trigger polypeptide copolymers thermogelled [40]. Jeong group ever found the pH-induced state change of block copolymers composed of PEG and poly(propylene glycol) (PPG) after introduction of a weak-acid moiety into the main chain in a multi-block form [41]. The carboxyl-capping of block copolymers of polyether and biodegradable polyester is reported first in the present paper by us. Each copolymer could then load just two charges in maximum, but still a significant change was found.

The phase diagram of our carboxyl-capped copolymer sample is shown in Fig. 4b. The solution did not undergo the sol–gel transition by increasing temperature at a high pH, therefore the cloud point was used to describe the aggregation behaviors. Comparison between Fig. 4a and b reveals that the cloud points of carboxyl-capped PLGA–PEG–PLGA are, at a low pH, much lower than those of the initial PLGA–PEG–PLGA, but much higher at a high pH. At a unionized state, even a little elongation of the copolymer due to end capping significantly changes the macroscopic state of a multi-chain system in a selective solvent because hydrophobicity of the whole polymer is enhanced; on the other hand, an ionization at a relatively high pH enhances the apparent hydrophilicity of the block copolymer and also changes its macroscopic state. Hence, an end group of such an amphiphilic block copolymer can tune its material property to a large extent.

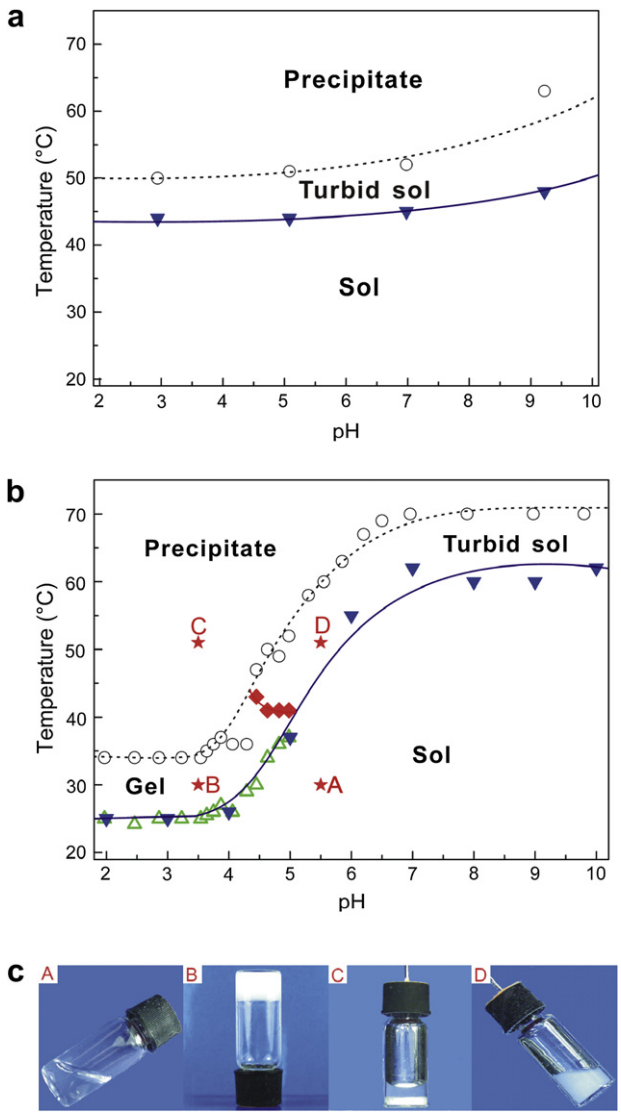

Fig. 4. Phase diagram of virgin PLGA–PEG–PLGA (a) and carboxyl-capped PLGA–PEG–PLGA copolymers (b) with different pH and temperature values. Polymer concentration is 20 wt%. Data points are from the inverted vial experiments and the cloud point experiments. In figure (a), filled inverted triangles (▼) represent the cloud point of PLGA–PEG–PLGA; hollow circles (○) represent the precipitation temperature of PLGA–PEG–PLGA; In Fig. 4(b), hollow triangles (△) represent the sol–gel transition temperature; filled inverted triangles (▼) represent the cloud point; filled diamonds (◆) represent the gel-(turbid sol) transition temperature; and hollow circles (○) represent the precipitation temperature. The filled stars (★) denote four typical states marked as A, B, C and D in the phase diagram, and the corresponding images are shown in Fig. 4(c) at the bottom representing sol, gel, precipitation and turbid sol, respectively. All lines in (a) and (b) are just for guidance of eyes.

The phase diagram of carboxyl-capped copolymer could be divided into four windows corresponding to sol, gel, precipitate, and turbid sol. The images in Fig. 4c indicate the four typical states with the pH and temperature conditions marked in (b) denoted by the star points marked as A, B, C, and D. The phase-transition behaviors of the aqueous solution of carboxyl-capped copolymers upon increase of temperature are influenced by medium pH, which could be divided into three pH regions as follows:

(1) *Sol–gel-precipitate transitions at a low pH.* When pH value was below 4.5, three states, sol, gel and precipitate were found with increase of temperature. The sol–gel transition was reversible if lowering temperature. The reverse transition happened after putting sample in a refrigerator at 4 °C overnight, even without help of stirring. The precipitate-to-gel transition upon decrease of temperature did not take place without help of stirring for a long time; but thermodynamically, this transition is still reversible, for the collected precipitate can be re-dissolved in water at low temperatures under stirring. Below pH 3.5, both the sol–gel transition temperature and the cloud point were close to 25 °C, the gel-precipitation transition occurred at about 34 °C; the height of gel window was then about 9 °C, and the sol–gel transition temperature was insensitive to pH in this sub-region. Between pH 3.5 and 4.5, the sol–gel transition temperature, the cloud point and the gel-precipitation temperature increased with pH.

(2) *Sol-(turbid sol)-precipitate transitions at a relative high pH.* When pH was higher than 5.0, the aqueous solution exhibited sol, flowable turbid sol, and precipitation states with increase of temperature. No gelling was observed any more, but a turbid sol was found. Between pH 5.0 and 7.0, the cloud point and the (turbid sol)-precipitation transition temperature increased with pH. Above pH 7.0, the cloud point and the turbid sol-precipitation transition temperature remained nearly a constant with increase of pH.

(3) *Sol–gel-(turbid sol)-precipitate transitions at a moderate pH.* The most complicated state transitions occurred at a moderate pH. All of the four states, sol, gel, flowable turbid sol, and precipitate were found in this region. Compared to the low-pH region, the gel could, following a sol–gel transition, become a flowable turbid solution at a higher temperature. While the sol–gel transition temperature and the turbid sol-precipitation temperature increased with pH, the transition temperature from gel to flowable turbid sol decreased a bit with increase of pH.

The quantitative rheological measurements indicated that the viscosity of carboxyl-capped PLGA–PEG–PLGA copolymer solution was tuned by pH and temperature (Fig. 5). The sol–gel transition temperature could be obtained from the abrupt increase of viscosity η as a function of temperature. The maximum viscosity could reach 200 Pa·s at 25 °C at pH 3.0, but just a few Pa·s around 52 °C at pH 9.0. The rheological measurement is consistent with the vial-tube observations to determine the phase diagram.

The previous studies of phase behaviors of PLGA–PEG–PLGA copolymers (with a different composition) and other amphiphilic block copolymers in water have revealed three states, sol, gel and

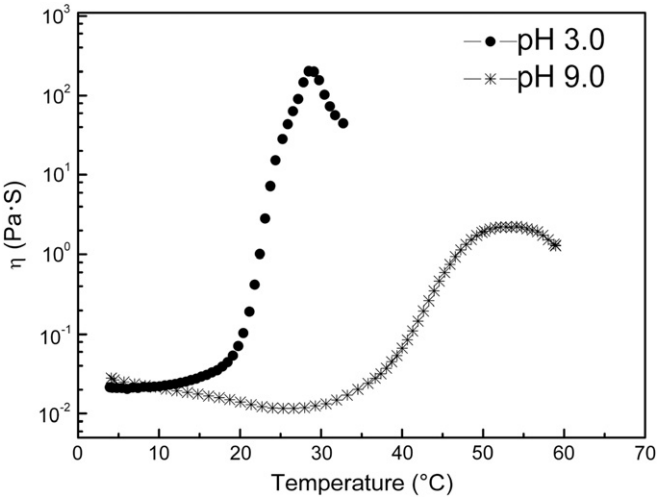

Fig. 5. Viscosity (η) of the 20 wt% carboxyl-capped PLGA–PEG–PLGA in PBS as a function of temperature at the marked two pH values. The heating rate was 0.5 °C/min.

precipitate [29,30]. The complicated transition among four states including the turbid sol as functions of both temperature and medium pH shown in Fig. 4 has, however, not yet been reported in the thermogelling neutral polyether-polyester block copolymers [7,8,11,13,21,22,29,30,35]. Lee group has also studied polyester-polyether derivatives ended with pH-sensitive moieties [20,21,42,43]. For instance, poly(ε-caprolactone-*co*-lactide)-poly (ethylene glycol) (PCLA–PEG) block copolymers were synthesized and extended by oligomeric sulfamethazine (OSM) to obtain OSM–PCLA–PEG–PCLA–OSM, and they successfully achieved significant pH- and temperature-sensitive physical gelling [21]. It should be indicated that the gelling condition in our sample as shown in Fig. 4 deviates from the normal physiological pH (7.4) and thus the present copolymer cannot be simply used as an injectable medical material, while some pH-sensitive thermogelling polymers invented by the Lee group can [20,21,42,44]. Nevertheless, the present study distinguishes itself by the finding of the fruitful macroscopic phase phenomena tuned by a very small end group and the following investigations of underling mesoscopic self-assembly behaviors.

3.4. pH dependent micellization behaviors

CMC was determined via the hydrophobic dye solubilization method. The results at two typical pH values are shown in Fig. 6. The CMC at pH 3.0 was a bit smaller than the sample at pH 9.0. Our detection indicates that even at a high pH, the 20 wt% solution could still form micelles, although it could not be gelled upon heating.

The micelle sizes of a concentration higher than CMC were measured by DLS and the results at different pH values are shown in Fig. 7. For instance, at pH 8.94, the average hydrodynamic radius of micelles $\langle R_h \rangle$ was 8.0 nm; at pH 3.02, $\langle R_h \rangle$ was 28 nm, leading to a 43-fold increase of volume. If we define the transition pH of the micelle sizes as pH*, the value could also be obtained via fitting with HH equation, resulting in pH* = 4.58. The transition pH region of micelle size in Fig. 7 is consistent with that of macroscopic phase states as shown in Fig. 4b.

The micelle morphology was observed via TEM, as shown in Fig. 8. At pH 3.0, the micelle was robust, and the diameter was about 40–60 nm. At pH 9.0, however, the micelle was loose and about 5–10 nm. The size difference between DLS and TEM is reasonable because DLS measures the hydrated micelle and TEM observes the dried samples [45]. TEM also straightforwardly confirmed that the carboxyl-capped PLGA–PEG–PLGA could form micelles at pH 9.0 as well.

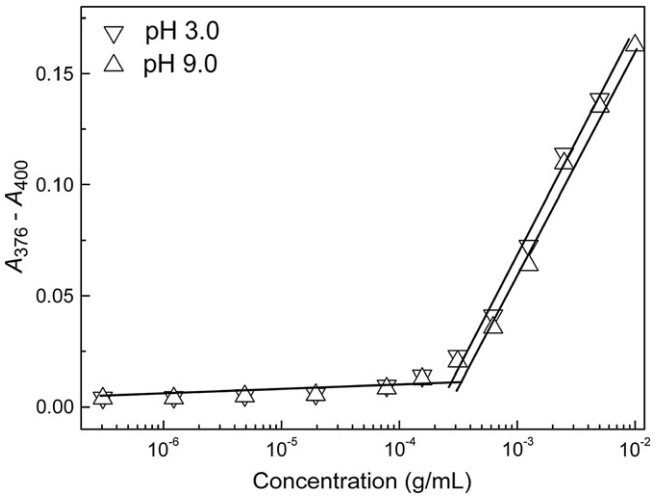

Fig. 6. Absorbance difference of 0.4 mM DPH at 376 nm and 400 nm as a function of polymer concentration. CMC reads 2.8×10^{-4} g/mL under pH 3.0 and 3.4×10^{-4} g/mL under pH 9.0.

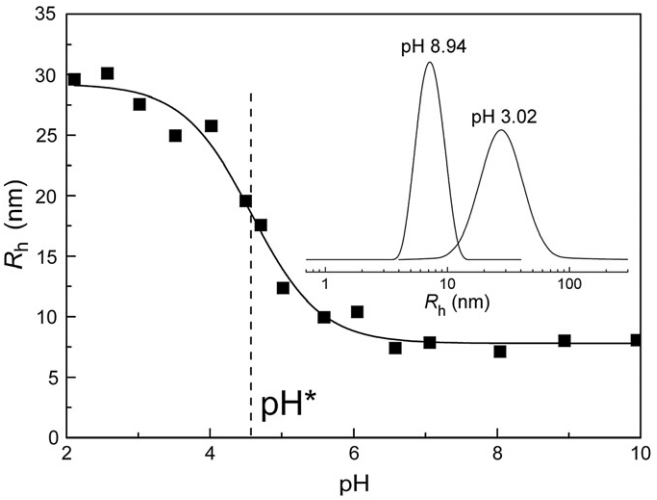

Fig. 7. Hydrodynamic radius of copolymer micelles in water (0.5 wt%) as a function of pH at 25 °C. The solid line is a fit from HH equation resulting in $pK_a = 4.58 \pm 0.08$, $n = -0.91 \pm 0.16$. The dashed line indicates pH*, the transition pH value. The inset shows two typical size distribution curves.

^{1}H NMR and ^{13}C NMR were employed to further investigate the effects of pH on the self-assembly of carboxyl-capped PLGA–PEG–PLGA in water. From Fig. 9(a), the signals assigned to the lactyl protons $-CH_3$ and the methylene protons $-CH_2CH_2-$ become broaden and less intense with decreasing pH. At pH 9.32, the micelles were loose, the PLGA segment and the carboxyl group had high mobility, thus the signals show narrow and strong resonance peaks in the ^{1}H NMR spectrum. At pH 2.38, the PLGA segment and the carboxyl group were buried in the micelles and had low mobility, so the signals were relatively broad. Such a trend was also reported by Yan group in studies of carboxyl-terminated hyperbranched polymers via ^{1}H NMR [37]. We further performed ^{13}C NMR experiments and observed a similar pH response as seen in Fig. 9(b). The NMR measurements (Fig. 9) are basically consistent with the TEM observations (Fig. 8).

It should be mentioned that the phenomenon of a decrease of micelle size with the increase of ionization degree was previously reported by Wu and Jiang groups in studies of carboxylated polystyrene ionomers [32–34]. They ever synthesized a series of carboxylated poly(styrene-*b*-ethylene-*co*-butylene-*b*-styrene) triblock copolymer, and checked the ratio of radius of gyration of micelles R_g over hydrodynamic radius R_h [33]. Although their

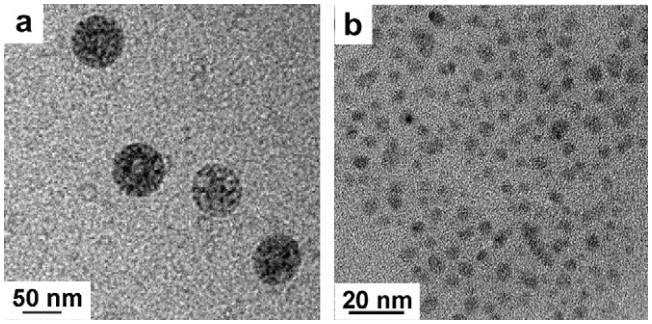

Fig. 8. TEM images of carboxyl-capped PLGA–PEG–PLGA at pH 3.0 (a) and pH 9.0 (b).

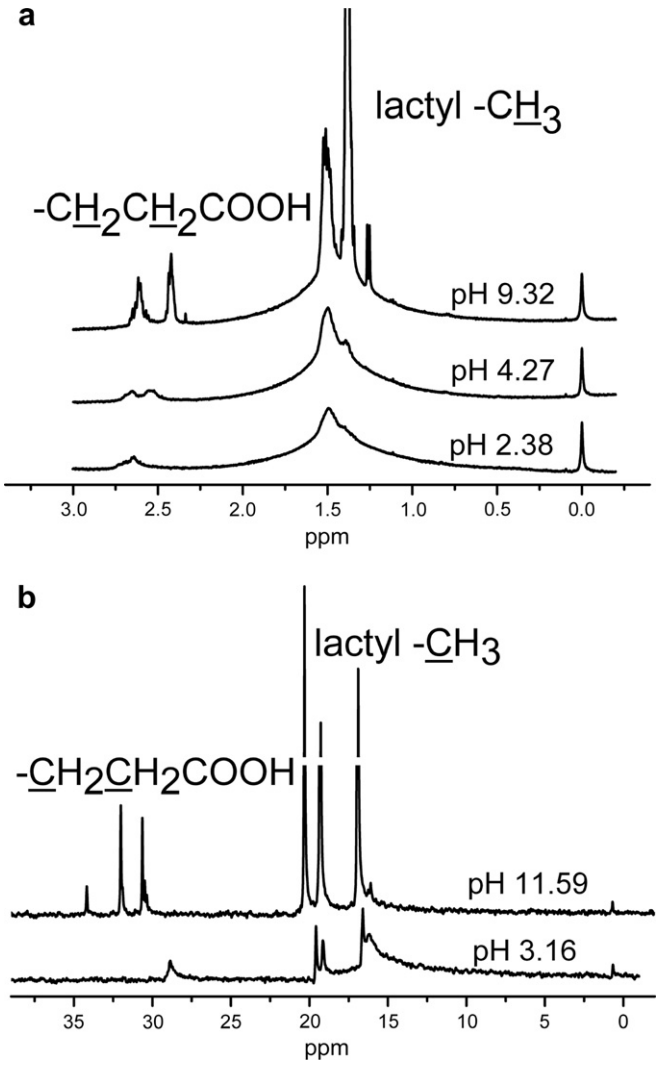

Fig. 9. ^{1}H NMR (a) and ^{13}C NMR (b) spectra of carboxyl-capped PLGA–PEG–PLGA solution (1 wt%) in D_2O at indicated pH values at 25 °C. The solution pH was adjusted by addition of DCl and NaOD.

carboxylation extent was not adjusted by medium pH but by introduction of more carboxylic groups into PS blocks via chemical reaction, their basic conclusion from scattering experiments that micelles with a high carboxylation extent were looser is useful for interpretation of our experimental phenomenon about pH dependence of micelles of our carboxyl-capped block copolymers. We herein afford more experimental evidences via TEM observations (Fig. 8) and NMR detections (Fig. 9).

3.5. Temperature dependent micellization behaviors

Temperature not only strengthens the effect of hydrophobic interaction on free energy, but also alters the ionization/deionization balance of the carboxy end groups. So it is meaningful to examine the effect of temperature on the self-assembly behaviors of carboxyl-capped PLGA–PEG–PLGA. Fig. 10 shows the average hydrodynamic radius of the micelles as a function of temperature. Interestingly, at pH 4.85, with the increase of temperature, the hydrodynamic radius of micelles exhibited a small peak at moderate temperatures before significantly aggregated at high temperatures. At the moment, we cannot give any detailed interpretation of the peak, and the polymer concentration in DLS measurement (0.2 wt% in Fig. 10) is also much lower than that in phase diagram determination (20 wt% in Fig. 4). But both measurements indicate complication of temperature dependence at a moderate pH.

4. Discussion

4.1. Complex of ionization degree and dissociation constant of weak-acid groups in amphiphilic polymer solution

4.1.1. Dependence of pK_a and α upon T

Temperature influences dissociation constant K_a and thus degree of ionization α. As is known,

$$pK_a = \frac{\Delta G(T)}{2.303RT}, \tag{6}$$

where $\Delta G(T)$ denotes the change of the Gibbs free energy in a dissociation process at temperature T, R is the molar gas constant. After neglecting temperature dependence of ΔG, we could, by combination of equations (4)–(6), get the relationship among α, pK_a and pH as

$$\alpha = \frac{1}{1 + 10^{n\left[-pH + (T_{ref}/T)pK_{a,ref}\right]}}, \tag{7}$$

Here, $pK_{a,ref}$ is pK_a at a reference temperature T_{ref}. T_{ref} and $pK_{a,ref}$ could be pre-determined. For simplicity, n is assumed to be a constant. Then at a given pH, the above equation only has two variables, α and T. Some of the theoretical calculation is demonstrated in Fig. 11. From the graph, at pH 2.98 or pH 7.76, temperature has little effect on the ionization degree, but a notable effect at moderate pH around $pK_a(0.5)$.

4.1.2. Dependence of pK_a upon α and pH

More significant complex comes from the α dependence and thus pH dependence of pK_a in our samples. In an ideal condition and thus neglecting difference between activity and concentration, combination of equations (1) and (2) leads to

$$pK_a = pH - \lg[\alpha/(1-\alpha)]. \tag{8}$$

This relation could be used to calculate pK_a at different pH values. The results of carboxylated PLGA–PEG–PLGA along with

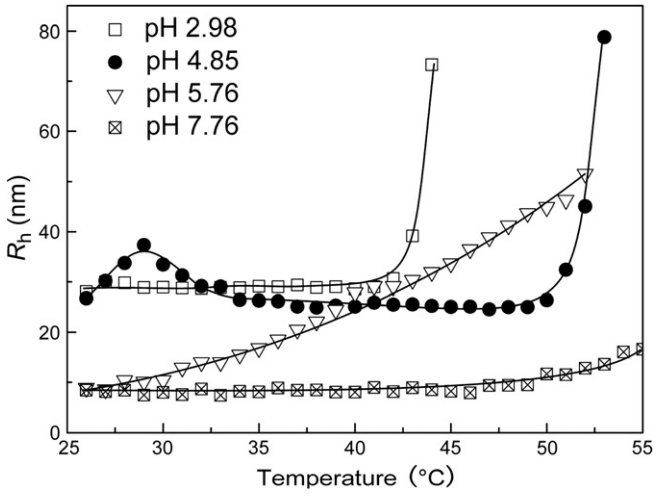

Fig. 10. Hydrodynamic radius of copolymer micelles in water (0.2 wt%) as a function of temperature at indicated different pH values. Each sample was equilibrated for 5 minutes at each temperature and then tested for 5 min. The lines are just for guidance of eyes.

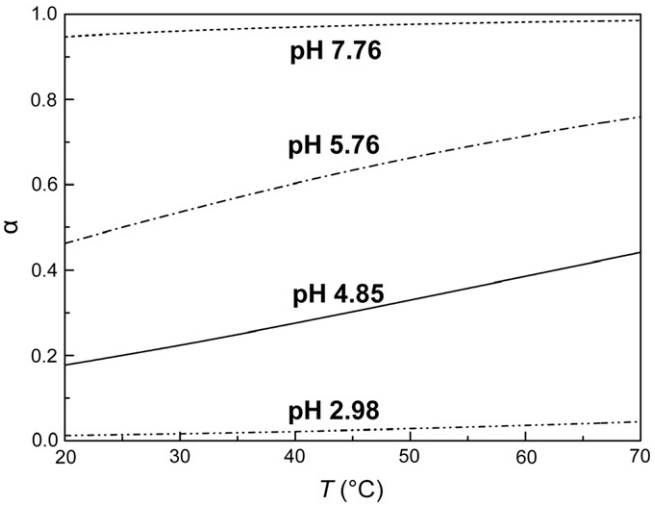

Fig. 11. Theoretical curves of degree of ionization (α) of the carboxyl-capped PLGA–PEG–PLGA in water as a function of temperature (T) at indicated pH values. The $pK_{a,ref}$ of the carboxyl end group was set as 5.85 at $T_{ref} = 20.5\,^{\circ}C$, and n was 0.66, as predetermined from Fig. 3.

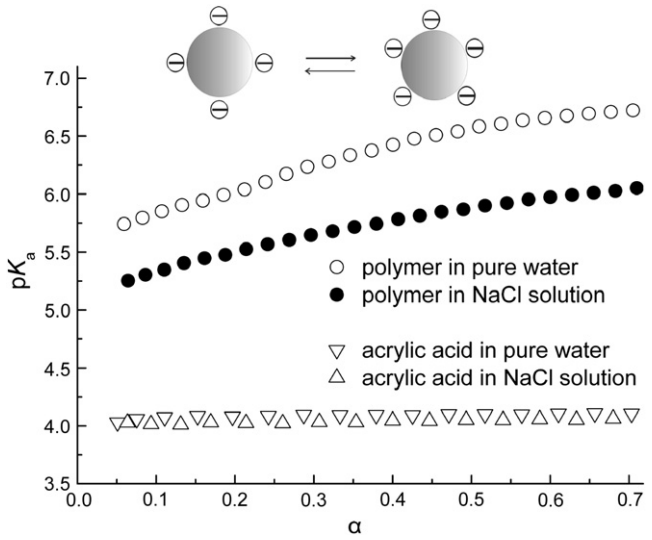

Fig. 12. pK_a as a function of α for 2 wt% (4.6 mM) HOOC–PLGA–PEG–PLGA–COOH or 0.2 wt% (28 mM) acrylic acid $CH_2CHCOOH$ in pure water or 0.9 wt% NaCl solution. The pK_a values were calculated via equation (8) based upon the α values obtained by equation (4). The inset presents schematically that the dissociation of a weak acid on the surface of a colloid might lead to the change of the electrostatic potential.

acrylic acid are shown in Fig. 12. While pK_a of the small molecular weak acid is almost pH-independent, the polymeric counterpart exhibits "abnormal" behaviors—pK_a is not a constant but significantly increased with pH or α.

The essential difference of our macromolecular samples from the small molecular counterpart comes from the micelle formation of the amphiphilic block copolymers. The dissociation of the weak acid leads to the change of surface charge of micelles. This effect might be more significant in our case where the carboxy groups are linked to the ends of hydrophobic blocks and thus the deionized groups might be located on the surface of cores, leading to a relatively high charge density. The change of the electrostatic potential in a dissociation process of a weak acid is not a constant with degree of ionization, so the dissociation constant is a function of medium pH. The process is even more complicated if ionization leads to any change of hydrophobic interaction. In this case, ΔG in equation (6) is divided into three parts, the "inherent" free energy difference at $\alpha = 0$, the change of electrostatic potential ΔG_{el}, the change of free energy due to a change of hydrophobicity-related entropy ΔS_{hy}. Then,

$$pK_a(\alpha, T) = pK_a(T)|_{\alpha=0} + \frac{\Delta G_{el}[\alpha(T)]}{2.303RT} + \frac{\Delta S_{hy}[\alpha(T)]}{2.303R}. \quad (9)$$

Hence, pK_a is not a constant again, and that is why the fitted pK_a in Fig. 3 is termed as $pK_a(0.5)$ by us. The ionization process must lead to an energy penalty due to increased repulsion among surface charges, as schematically presented in the inset of Fig. 12. So, pK_a is increased with α (and thus with pH for our polymeric sample). The significant decrease of pK_a under a saline environment in the case of polymer samples might be accounted for from the screening of electrostatic potential to a certain extent. The dependence of pK_a upon α and salt agree with the previous reports in studies of other macromolecular samples containing weak-acid groups [38]. The decrease of pK_a of a macromolecular weak acid under saline solutions was also consistent well with the measurements of proteins called bacteriorhodopsin and archaerhodopsin by our group [39]. In fact, the change of pK_a of the so-called proton release complex adjusted by microenvironment plays a vital role in the proton pumping activity of the retinal proteins [46].

It seems worthy of mentioning that early in 1993 Urry et al. found significant electrostatic- and hydrophobic-induced shifts of pK_a of aspartic acid residues (Asp) in a series of polypentapeptides with different Asp fraction f_D [47]. The pK_a was found to be increased upon addition of salt when $f_D < 0.65$ while decreased when $f_D > 0.65$. They concluded that the charge-charge repulsion was predominant at high Asp content and the effect of hydrophobic interaction was predominant at low Asp content. Considering that salts lowered pK_a in our polymeric sample as shown in Fig. 12, the electrostatic interaction must be significant due to a screening effect, although there is no reason at the moment to exclude the direct hydrophobic interaction completely.

The effects of the hydrophobic interaction on pK_a come from two aspects: one is indirect; the other is direct as reflected in the third term in equation (9). The indirect one works in most of relevant cases because the hydrophobic interaction leads to the micelle formation in water and it is the electrostatic potential on the surface of colloids that rationalizes the second term in equation (9). The direct hydrophobic effect on pK_a of an amphiphilic polymeric electrolyte or ionomer might come from the disturbance of hydration shells of ionizable groups and nearby nonpolar groups. The underlying mechanism remains to be further confirmed, and a corresponding theoretical treatment is called for.

4.2. The physical picture of multi-scale self-assembly of carboxyl-capped PLGA–PEG–PLGA chains in water

In our previous paper, formation of a percolated micelle network was suggested to account for the physical thermogelling of the polyester-polyether block copolymers [17,30,35,48]. As the carboxy group was introduced to the end of PLGA–PEG–PLGA, the micellization and gelation behaviors in water might be reasonably affected by both temperature and pH. This complication did be observed. Based upon the analyses above, the physical pictures of the self-assembly of carboxyl-capped PLGA–PEG–PLGA on different scales are presented in Fig. 13.

Basically, medium pH significantly affects micellization and then gelation behaviors of the carboxyl-capped PLGA–PEG–PLGA in water. In accordance of the phase diagram shown in Fig. 4b, we discuss here the physical pictures in three pH regions.

(1) *Sol–gel-precipitate transitions at a low pH*. Below pH 4.5, most of the carboxy groups were not ionized and acted as hydrophobic groups, and the unionized carboxyl groups may trend to form hydrogen bonding [37]. More importantly, the hydrophobic blocks are, as shown in Fig. 1, then a bit longer, which might lead to significant effects on macroscopic condensed state [30,35]. So, not only could the carboxyl-capped PLGA–PEG–PLGA self-assemble into micelles, but also the relatively big and robust micelles further self-assemble into a percolated micelle network and thus a hydrogel with increase of temperature. The hydrogel might be dehydrated at a higher temperature. In this pH region, a concentrated carboxyl-capped PLGA–PEG–PLGA aqueous sample exhibits sol, hydrogel and precipitation states. Transitions from A to B to C were hence observed in Fig. 4b and illustrated in Fig. 13.

(2) *Sol-(turbid sol)-precipitate transitions at a relative high pH*. Above pH 5.0, many ionized carboxy groups were sufficiently hydrophilic and surrounded by an electric double layer. Although polymers could still self-assemble into micelles, the micelles were loose and small, as illustrated by Figs. 7 and 8. The micelles are then difficult to form a network with an infinite correlation, and could thus only be aggregated into a turbid sol. Then, transitions from A to D to C were hence observed in Fig. 4b and illustrated in Fig. 13.

(3) *Sol–gel-(turbid sol)-precipitate transitions at a moderate pH*. Between pH 4.5 to pH 5.0, the carboxy groups were partially ionized, and frequently shift between hydrophobic/neutral state and hydrophilic/charged state in a dynamic equilibrium. The ionization degree is very sensitive to temperature in this pH region, as schematically shown in Fig. 11. We herein rewrite the well known the 2nd law of thermodynamics as

$$\Delta G[T, \alpha(\mathrm{pH}, T)] = \Delta H[\alpha(\mathrm{pH}, T)] - T\Delta S[\alpha(\mathrm{pH}, T)]. \quad (10)$$

Here, G, H and S denote free energy, enthalpy and entropy, respectively. The association of amphiphilic block copolymers is predominant only if $\Delta G < 0$. From this point of view, an increase of T is beneficial for micelle aggregation because the hydrophobic interaction is an entropy effect coming from water orientation around the surface of a hydrophobic group or segment. On the other hand, a rise of temperature increases the ionization degree of the carboxy group significantly at a moderate pH and thus increases the ionization degree to a certain extent, which leads to a decrease of hydrophobicity of the copolymer. Then, the positive ΔS in an association process is decreased with increase of T, and micelles might become smaller and looser due to more hydrophilicity and surface stabilization of charges.

So, a temperature rise leads to two opposite trends, the decrease of hydrophobicity due to an increased ionization degree and the apparent enhancement of the contribution of an entropy effect to the global free energy. Such an interplay is very subtle at a moderate pH, in which the dependence of α upon T is significant and nonlinear. The micelle sizes could possibly be increased first and then decreased in heating sometimes as shown in Fig. 10. As

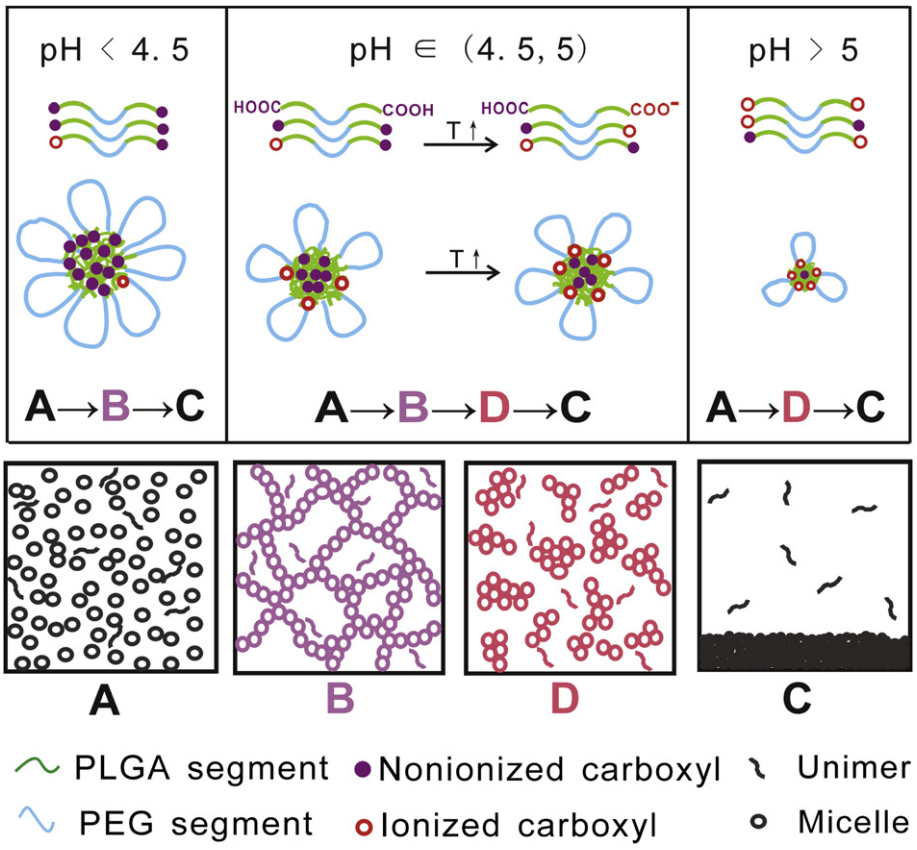

Fig. 13. Schematic illustration of ionization and self-assembly of carboxyl-capped PLGA–PEG–PLGA copolymers into micelles and hydrogels at varied pH and temperature. The upper and middle-upper parts illustrate ionization degree of the end groups of block copolymer chains and the micelle structures at the three pH regions; the temperature effect on ionization is also significant at the moderate pH region. The internal structures of the four macroscopic states, sol, gel, precipitate and turbid sol are presented in the lower part with the symbols of A, B, C and D identical to Fig. 4. The state transitions at each pH region upon an increase of temperature are indicated by the arrows in the middle part.

a result, a concentrated carboxyl-capped PLGA–PEG–PLGA solution might undergo sol-to-hydrogel-to-turbid-sol-to-precipitation transitions in Fig. 4, which is illustrated in Fig. 13 as A → B → D → C. It could also be understood that the sol–gel transition temperature possibly increased above pH 4.0, and even disappeared above pH 5.0.

4.3. The transition pH values of mesostructure and macrostate are unnecessary equal to pK_a of the carboxylate polymer

The pH-related behaviors of an electrolyte must be closely related to the ionization states of the corresponding ionizable groups. Even though only one kind of weak acidic group was introduced into our macromolecules, we found that the moderate pH in the transition region (Fig. 4b) significantly deviate from the transition pH of ionization of carboxylated polymers (Fig. 3), while the mesoscopic and macroscopic transitions happened in the similar pH region (comparison between Figs. 4b and 7). The pH^* from Fig. 7 (4.58) is not close to $pK_a(0.5)$ (5.85). The phenomenon that an abrupt change of micelle sizes did not happen at $\alpha = 0.5$ was also reported by others in studies of pH-sensitive micelles of other polyelectrolytes in water [49,50]. According to Fig. 3b, the degree of ionization at pH^* is only about 0.13, at which 87–74% copolymers are still not charged. Despite of a different polymer concentration of titration in Fig. 3 from that of state observation in Fig. 4b, we could conclude that the critical degree of ionization for phase transition in our polymeric sample might be significantly less than 50%. Further considering just two weak acid groups in a macromolecular chain in our experiments, our research reveals that a bit ionization could lead to a significant mesoscopic and macroscopic change.

5. Conclusions

A pH-sensitive block copolymer was obtained by introducing carboxy groups into the two ends of PLGA–PEG–PLGA. Vial-tube observation, acid-base titration, DLS, TEM, ^{1}H NMR, ^{13}C NMR, hydrophobic dye solubilization and rheological measurements were performed to investigate the self-assembly behaviors of carboxyl-capped PLGA–PEG–PLGA in water as functions of pH and temperature. The virgin copolymer with the composition synthesized in this paper did not undergo sol–gel transition upon increase of temperature. We found, however, that a bit elongation of the virgin polymer with just a small end group led to a surprisingly drastic effect on the macroscopic states of polymers in water. The aqueous solution of the end-capped copolymer exhibited four states, sol, gel, precipitate, and turbid sol, depending upon pH and temperature. At moderate temperatures, three reversible transitions were found including sol-to-gel, gel-to-(turbid sol), and (turbid sol)-to-precipitate transitions. A mesoscopic interpretation to the macroscopic phase transitions was further preliminarily put forward. The interplay of two opposite effects accounts for the complex of temperature dependence of micelle sizes and macroscopic states at a moderate pH. The complex of α and pK_a of amphiphilic macromolecules with ionizable groups is strengthened. Although each copolymer can only load two negative charges at most in our samples, the very delicate effects of ionizable groups on both mesoscopic and macroscopic behaviors are revealed. The research shed some insight into the multi-scale self-assembly of amphiphilic block copolymer ionomers. Our studies also imply the potential of molecular design of new wet materials by introducing a few weak-acidic or weak-basic groups into polymer chains.

Acknowledgements

The authors thank the financial supports by Chinese Ministry of Science and Technology (973 Program No. 2009CB930000), NSF of China (Grant Nos. 50533010 and 20774020), Science and Technology Developing Foundation of Shanghai (Grant Nos. 07JC14005, No. 074319117 and No. 09ZR1403700), and Shanghai Education Committee (Project No. B112).

References

[1] Zhang LF, Eisenberg A. Science 1995;268:1728–31.
[2] Jeong B, Bae YH, Lee DS, Kim SW. Nature 1997;388:860–2.
[3] Rodriguez-Hernandez J, Checot F, Gnanou Y, Lecommandoux S. Prog Polym Sci 2005;30:691–724.
[4] Licciardi M, Giammona G, Du JZ, Armes SP, Tang YQ, Lewis AL. Polymer 2006;47:2946–55.
[5] Ji SC, Ding JD. Langmuir 2006;22:553–9.
[6] Kadam VS, Badiger MV, Wadgaonkar PP, Ducouret G, Hourdet D. Polymer 2008;49:4635–46.
[7] Jeong B, Kibbey MR, Birnbaum JC, Won YY, Gutowska A. Macromolecules 2000;33:8317–22.
[8] Zentner GM, Rathi R, Shih C, McRea JC, Seo MH, Oh H, et al. J Control Release 2001;72:203–15.
[9] Zhou Z, Chu B. Macromolecules 1994;27:2025–33.
[10] Alexandridis P, Holzwarth JF, Hatton TA. Macromolecules 1994;27:2414–25.
[11] Jeong B, Bae YH, Kim SW. Colloids Surf B Biointerfaces 1999;16:185–93.
[12] Jeong B, Kim SW, Bae YH. Adv Drug Deliv Rev 2002;54:37–51.
[13] Chung YM, Simmons KL, Gutowska A, Jeong B. Biomacromolecules 2002;3:511–6.
[14] Xiong XY, Tam KC, Gan LH. Polymer 2005;46:1841–50.
[15] Bae SJ, Suh JM, Sohn YS, Bae YH, Kim SW, Jeong B. Macromolecules 2005;38:5260–5.
[16] Jiang ZQ, You YJ, Deng XM, Hao JY. Polymer 2007;48:4786–92.
[17] Zhang H, Yu L, Ding JD. Macromolecules 2008;41:6493–9.
[18] Yu L, Ding JD. Chem Soc Rev 2008;37:1473–81.
[19] He CL, Kim SW, Lee DS. J Control Release 2008;127:189–207.
[20] Huynh DP, Nguyen MK, Pi BS, Kim MS, Chae SY, Kang CL, et al. Biomaterials 2008;29:2527–34.
[21] Shim WS, Kim SW, Lee DS. Biomacromolecules 2006;7:1935–41.
[22] Park SY, Lee Y, Bae KH, Ahn CH, Park TG. Macromol Rapid Commun 2007;28:1172–6.
[23] Li L, Lim LH, Wang QQ, Jiang SP. Polymer 2008;49:1952–60.
[24] Jeong B, Lee KM, Gutowska A, An YHH. Biomacromolecules 2002;3:865–8.
[25] Yu L, Chang GT, Zhang H, Ding JD. Int J Pharm 2008;348:95–106.
[26] Van Tomme SR, Storm G, Hennink WE. Int J Pharm 2008;355:1–18.
[27] Hoare TR, Kohane DS. Polymer 2008;49:1993–2007.
[28] Chen JP, Cheng TH. Polymer 2009;50:107–16.
[29] Lee DS, Shim MS, Kim SW, Lee H, Park I, Chang TY. Macromol Rapid Commun 2001;22:587–92.
[30] Yu L, Chang GT, Zhang H, Ding JD. J Polym Sci, Polym Chem 2007;45:1122–33.
[31] Yu L, Zhang Z, Zhang H, Ding JD. Biomacromolecules 2009;10:1547–53.
[32] Li M, Zhang YB, Jiang M, Zhu L, Wu C. Macromolecules 1998;31:6841–4.
[33] Zhang GZ, Liu L, Zhao Y, Ning FL, Jiang M, Wu C. Macromolecules 2000;33:6340–3.
[34] Liu SY, Hu TJ, Liang HJ, Jiang M, Wu C. Macromolecules 2000;33:8640–3.
[35] Yu L, Zhang H, Ding JD. Angew Chem Int Ed 2006;45:2232–5.
[36] Yusa S, Sakakibara AK, Yamamoto T, Morishima Y. Macromolecules 2002;35:5243–9.
[37] Dong WY, Zhou YF, Yan DY, Li HQ, Liu Y. Phys Chem Chem Phys 2007;9:1255–62.
[38] Kawaguchi S, Yekta A, Winnik MA. J Colloid Interface Sci 1995;176:362–9.
[39] Wu J, Ma DW, Wang YZ, Ming M, Balashov SP, Ding JD. J Phys Chem B 2009;113:4482–91.
[40] Kim JY, Park MH, Joo MK, Lee SY, Jeong B. Macromolecules 2009;42:3147–51.
[41] Suh JM, Bae SJ, Jeong B. Adv Mater 2005;17:118–20.
[42] Dayananda K, He C, Park DK, Park TG, Lee DS. Polymer 2008;49:4968–73.
[43] Huynh DP, Nguyen MK, Kim BS, Lee DS. Polymer 2009;50:2565–71.
[44] Nguyen MK, Huynh CT, Lee DS. Polymer 2009. doi:10.1016/j.polymer.2009.09.040.
[45] Wan S, Jiang M, Zhang GZ. Macromolecules 2007;40:5552–8.
[46] Ming M, Lu M, Balashov SP, Ebrey TG, Li QG, Ding JD. Biophys J 2006;90:3322–32.
[47] Urry DW, Peng SQ, Parker TM, Gowda DC, Harris RD. Angew Chem Int Ed 1993;32:1440–2.
[48] Yang ZG, Ding JD. Macromol Rapid Commun 2008;29:751–6.
[49] Lee AS, Gast AP, Butun V, Armes SP. Macromolecules 1999;32:4302–10.
[50] Vamvakaki M, Palioura D, Spyros A, Armes SP, Anastasiadis SH. Macromolecules 2006;39:5106–12.